Hindawi

Research Article

Chitosan-Coated Solid Lipid Nano-Encapsulation Improves the Therapeutic Antiairway Inflammation Effect of Berberine against COPD in Cigarette Smoke-Exposed Rats

Hongxiang Liu [iD],[1] **Yifan Li** [iD],[1] **Xiaoying Zhang** [iD],[2] **Man Shi** [iD],[3] **Dexu Li** [iD],[1] **and Ying Wang** [iD][1]

[1]*Department of Integrated Chinese and Western Medicine, Affiliated Hospital of Hebei University, Baoding 071000, China*
[2]*Graduate School, Hebei University, Baoding 071000, China*
[3]*Department of Cardiology, Affiliated Hospital of Hebei University, Baoding 071000, China*

Correspondence should be addressed to Dexu Li; dexu.li2020@gmail.com and Ying Wang; 13582256313@sina.cn

Berberine (Ber) is an isoquinoline alkaloid that has shown therapeutic potential in mice with chronic obstructive pulmonary disease (COPD). However, the therapeutic efficiency of Ber is restricted by its low aqueous solubility and bioavailability. Chitosan and solid lipid nanoparticles (SLNs) have demonstrated great abilities as delivery systems in enhancing the bioavailability of therapeutic compounds. The present study aimed to get together the biological features of SLNs with the advantages of chitosan to formulate an efficient nano-carrier platform for the oral delivery of Ber and evaluate the therapeutic effect of the prepared Ber-encapsulated nanoparticles on airway inflammation in cigarette smoke (CS)-induced COPD rats. The Ber-encapsulated SLE-chitosan formulation was manufactured using a modified solvent-injection method followed by a homogenization process. Physicochemical properties, encapsulation efficiency, in vitro stability and Ber release, and pharmacokinetics of the manufactured formulation were evaluated. The COPD rat model was developed by exposing animals to CS. To study the therapeutic efficiency of Ber-encapsulated SLE-chitosan nanoparticles and pure berberine, the histopathological changes of the lung tissues, levels of inflammatory cells and cytokines, and activities of myeloperoxidase (MPO) and superoxide dismutase (SOD) enzymes were evaluated in bronchoalveolar lavage fluid (BALF). Ber-encapsulated SLE-chitosan showed the particle size in nano-range with high stability and controlled slow-release profile *in vitro* in simulated gastric (pH 1.5) and intestinal (pH 6.8) fluids. Administration of Ber-loaded SLE-chitosan nanoparticles could significantly ameliorate inflammation scores in lung tissues and reduce levels of inflammatory cells (neutrophils and macrophages) and inflammatory cytokines (IL-1β, Il-6, Il-17, and TNFα) in BALF when compared with the pure Ber. SLE-chitosan-based nanoparticles can strongly improve the therapeutic anti-inflammatory impact of Ber against CS-induced airway inflammation in COPD rats, suggesting the promising application of Ber-encapsulated SLN-chitosan nanoparticles for treating COPD and other inflammation-mediated diseases.

1. Introduction

Chronic obstructive pulmonary disease (COPD) is a progressive inflammatory disease involving the lung parenchyma and small airways, with chronic airway inflammation, resulting in luminal obstruction, the airway wall thickening via an elevation in mesenchymal cell proliferation and deposition of matrix molecules, and the airway narrowing by fibrosis, leading to a progressive decline in the lung activity [1]. Cigarette smoke (CS), which contains endotoxins and thousands of oxidants inducing oxidative stress and inflammation in the lungs, is a well-documented etiological factor in COPD development [2, 3]. The long-term CS exposure triggers consistent airway inflammatory response and high oxidative stress status, which results in damage to the airway epithelium, airway mucus hypersecretion, and airway obstruction, eventually in a progressive airway narrowing and difficulty in breathing [2, 3]. Of note, chronic inflammation, including immune cells responses and inflammatory cytokines release, is the principal
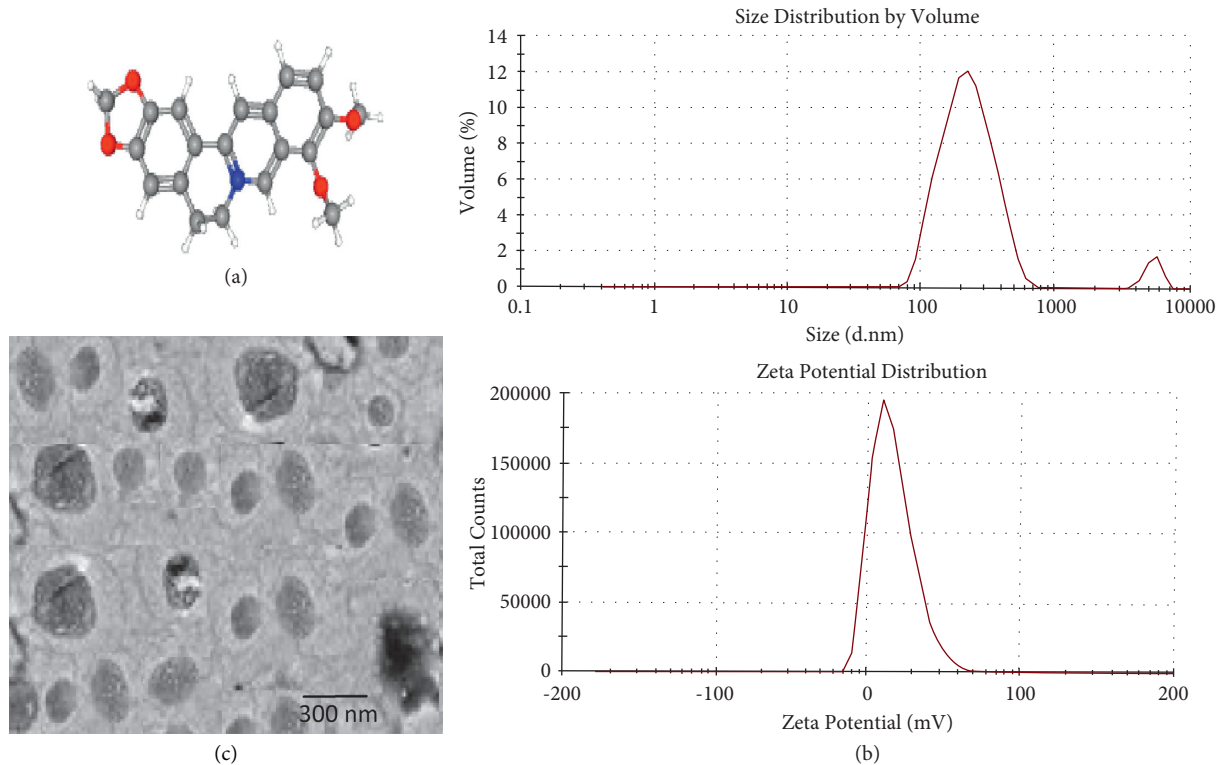
FIGURE 1: Physiochemical feature of Ber-loaded SLN-chitosan nanoparticles. (a) The chemical structure of berberine. (b) Nanoparticle size distribution and zeta potential. (c) TEM image of prepared Ber-loaded SLN-chitosan nanoparticles.

mechanism underlying the pathogenesis of CS-induced COPD. The CS-mediated inflammation is manifested by a number of immune cells such as neutrophils and macrophages as part of the inflammatory responses leading to alterations in several inflammatory mediators, such as tumor necrosis factor (TNF)-α, interleukin (IL)-1β, and IL-6, the levels of which are markedly elevated in COPD patients. Notably, CS triggers the activation of alveolar macrophages, which, with the aid of chemoattractants, lead to the infiltration of inflammatory cells, in particular neutrophils. The neutrophils eventually lead to the protease activation that causes the destruction of alveolar cells and connective tissue in the lung, as well as mucus hypersecretion, thereby inducing emphysema [2]. CS can also produce a large number of reactive oxygen species (ROS) that exacerbate inflammatory responses and the destruction of lung tissue. CS is not only one of the exogenous ROS but also promotes inflammatory cells and the airway epithelial cells to generate large numbers of endogenous ROS [4, 5]. Thus, anti-inflammatory therapy and targeting oxidative stress with antioxidants are choices for COPD treatment. Inhaled corticosteroids are the main therapies for COPD, but numerous clinical studies have shown that they might exert potential side effects including hyperglycemia, cataracts, pneumonia, thrushosteoporosis in the upper airway, and dysphonia [6–8]. Hence, there is a need for exploring alternative or adjuvant agents with anti-inflammatory and antioxidant features ameliorating airway inflammation in COPD patients.

Berberine, a yellowish isoquinoline alkaloid (5, 6-dihydro-9, 10-dimethoxybenzo [g]-1, 3-benzodioxolo [5, 6-a] quinolizinium chloride, Figure 1(a)), is the main effective pharmacological component found in the stem bark and roots of the Chinese medicinal herb *Coptis chinensis* [9]. Berberine has been widely applied in Ayurveda and traditional Chinese medicine to treat sicknesses such as inflammation, hypertension, and intestinal infections [10]. In addition, berberine shows various pharmacological properties such as antitumor, anti-inflammation, immune modulation, and anti-oxidation [11–17]. Of note, increasing investigations pay attention to the impacts of berberine on pulmonary diseases and demonstrated that berberine could ameliorate CS-induced airway inflammation in mice [18–20]. Despite its therapeutic advantages, the clinical use of berberine in oral administration is restricted mainly due to low aqueous solubility and gastrointestinal absorption, rapid metabolism, and short biological half-life, which result in poor plasma levels and low bioavailability [21–23]. Of note, berberine is a hydrophilic compound that is categorized as a Class III drug in the biopharmaceutical classification system [24]. Class III drugs are hydrophilic and show low membrane permeability. These drugs are mainly absorbed through the paracellular pathway, which restricts intestinal absorption and results in poor bioavailability [25]. The low oral bioavailability of berberine can be due to various reasons: (1) self-aggregation of berberine, which reduces its solubility in the gastrointestinal fluids; (2) the first-pass effect both in the

liver and in the intestine; (3) its low permeability through the intestinal mucus layer [26]. On the other hand, high doses of berberine (0.9–1.5 g/day) can lead to gastrointestinal adverse effects, including stomach upset, cramping, and shaping gut microbiota, because of its low absorption and long-time administration [21–23]. To circumvent such limitations, the development of a delivery platform for the sustained release of berberine is needed to elevate its bioavailability by decreasing the dissolution rate in gastric media and also by enlarging the residence time in the intestinal mucus.

Recently, the use of solid lipid nanoparticles (SLNs) as delivery systems in enhancing the absorption of natural therapeutic compounds in traditional Chinese medicine has widely been investigated [26]. As potential drug carriers, SLNs have acquired considerable attention in recent years due to their remarkable advantages such as enhancing solubility and bioavailability of both hydrophilic and lipophilic agents, low toxicity and immunogenicity, inducing pharmacological activity, protecting the drugs from digestive enzymes, possessing significant biocompatibility and biodegradability, and being easy to formulate and of low price [27]. Of note, the integrity and stability of an oral drug delivery formulation in gastrointestinal media are of significant importance to provide *in vivo* efficacy. Although SLNs show an encouraging capability as an oral delivery system because of the high stability against digestive enzymes, the low stability of SLNs in the acidic condition of the stomach restricts clinical applications. To elevate the stability and absorption rate of SLNs, biopolymer coating has been used to formulate SLNs with sustained-release profiles and improved stability and mucoadhesive ability. Biopolymers with considerable mucoadhesive features and resistance to the acidic pH, such as chitosan, are excellent candidates to coat SLNs [28]. Chitosan is a chitin-derived cationic polysaccharide that, once is added to the surface of nanoparticles, can elevate the uptake of the encapsulated agents by the mucosal surface [29]. Moreover, under the acidic pH, chitosan is protonated and firmly interacts with negatively charged SLNs, consequently forming well-organized and stable delivery platforms, together with providing a sustained release of the encapsulated compound [30]. Thus, using the chitosan coating protects SLNs against the stringent medium of the gastrointestinal tract and improves their transmucosal delivery, thereby elevating the effective concentration of encapsulated compounds at the absorption site. Notably, chitosan-coated SLNs have been frequently shown to significantly enhance the absorption of various encapsulated drugs *in vivo* by increasing their residence time on the mucosa because of improved mucoadhesive features [30–33]. The present study aimed to get together the biological features of SLNs with the advantages of chitosan to formulate a new nano-carrier platform for the oral delivery of berberine and found that encapsulating in chitosan-coated SLNs could significantly improve the oral bioavailability and therapeutic efficiency of berberine in CS-induced COPD rats.

2. Materials and Methods

2.1. Preparation of Ber-Encapsulated SLN-Chitosan Nanoparticles.
Ber-encapsulated SLN-chitosan formulation was manufactured using a modified solvent-injection method [34], followed by a high-pressure homogenization process [35]. In brief, 40 mg of the solid lipid Witepsol 85E (triglycerides of C 10–C 18 saturated fatty acids) and 50 mg of berberine were dissolved in 1 mL of mixed solution composed of ethanol and acetone in equal ratios (1:1 v/v) at 75°C in a water bath until appearing an optically clear dispersion. To prepare Ber-encapsulated SLN nanoparticles coated with chitosan, the clear organic phase (the solid lipid-containing berberine) was injected into 20 mL of the hot aqueous phase preheated to the same temperature containing the emulsifier (pluronic as stabilizing surfactant) and chitosan at the concentrations of 2.5 mg/mL and 0.5 mg/mL, respectively, in double-distilled water. The mixture was emulsified under high agitation (25000 rpm for 4 min) at 70°C and then homogenized at the same temperature by applying six homogenization cycles at 800 bar using a high-pressure homogenizer (Panda 2k, Niro Soavi, Italy). The homogenized suspension was immediately cooled in an ice water bath to maintain the stability of the prepared Ber-encapsulated SLN-chitosan nanoparticles. The Ber-encapsulated SLN-chitosan suspension was filtered through a 0.45 μm filter and then freeze-dried.

2.2. Characterization of the Prepared Nanoparticles

2.2.1. Physiochemical Properties.
Physiochemical properties of the prepared nanoparticles, including the particle size (Z-average diameter), polydispersity index (PDI), and zeta potential (surface charge), were measured using a dynamic light scattering (DLS) instrument (Zetasizer, Malvern Instruments Ltd., Malvern, UK) at 25°C. The morphology of Ber-encapsulated SLN-chitosan nanoparticles was visualized by a transmission electron microscope (TEM, Hitachi H-600, Tokyo, Japan) after negative staining. In brief, one drop of nanoparticle suspension was spread onto a carbon film-coated copper grid (300 mesh) and then air-dried through 5 min incubation in a desiccator at room temperature. After drying, one drop of 1% (w/v) phosphotungstic acid solution was added to the grid for negative staining. Finally, the sample grids were air-dried at room temperature before TEM investigation.

2.2.2. Measuring Encapsulation Efficiency.
To determine the entrapment of berberine in chitosan-coated SLN suspension, the encapsulation efficiency (EE) was measured by evaluating the concentration of unencapsulated (free) berberine using the centrifugal ultrafiltration technique followed by the high-performance liquid chromatography (HPLC) method. To separate the unencapsulated berberine, the Ber-encapsulated SLN-chitosan suspension was centrifuged for 25 min at 22,000 rpm and 4°C. The concentration of free berberine in the liquid supernatant was then measured by HPLC on a Shimadzu (CBM 20A) system with a multi-

wavelength UV-VIS detector (SPD-20AV) equipped with a C18 reverse-phase column, 4.6 mm × 25 cm (Shimadzu, Japan). Finally, the EE of the nanoparticles was measured from the concentration of encapsulated berberine to the total concentration of initially added berberine. The encapsulated amount of berberine was calculated by subtracting the berberine concentration quantified by HPLC from the concentration of initially added berberine. The EE (%) was calculated by the following equation [36]: EE (%) = $(C_0 - C)/C_0 \times 100\%$, where C_0 is the total concentration of berberine initially added into the nanoparticle suspensions and C is the concentration of encapsulated berberine.

2.2.3. In vitro Stability.
The stability of Ber-encapsulated SLN-chitosan nanoparticles was evaluated when exposed to simulated intestinal fluid (SIF, pH 6.8) and simulated gastric fluid (SGF, pH 1.5). Ber-encapsulated SLN-chitosan nanoparticles were loaded to SIF and SGF and then incubated at 37°C for 6 h and 2 h, respectively. These time periods were employed based on the predicted homing time in the stomach and intestine. Particle size and EE % were measured at the aforementioned time intervals.

2.2.4. In Vitro Drug Release.
In vitro drug release was carried out in SIF and SGF to simulate the physiological conditions following oral administration. Ber-encapsulated SLN-chitosan nanoparticles were incubated at 37°C under continuous shaking at 100 rpm with SIF or SGF in separate microcentrifuge tubes. Ber-encapsulated SLN-chitosan nanoparticles were isolated by ultrafiltration-centrifugation using millipore ultrafiltration-centrifuge tubes (MWCO = 5 kDa). Finally, the ultrafiltrated samples were analyzed for measuring the berberine level using the already explained HPLC method [37].

2.3. COPD Rat Model Development and Treatment Protocol.
Male Sprague–Dawley (SD) rats, 6 weeks old, weighing 210 ± 25 g, were housed under the pathogen-free condition, at the controlled humidity (55 ± 5%) and temperature (24 ± 2°C), under a 12-hour dark/light schedule, with free access to water and food. After a 4-day acclimation, rats were randomly divided into the following groups ($n = 10$ per group) and treated daily. The Control group was exposed to room air and only received berberine-free SLN-chitosan nanoparticles. In the CS group, rats were intragastrically received berberine-free SLN-chitosan nanoparticles 1 h before CS exposure. In the Ber + CS group, rats were intragastrically treated with the aqueous suspension of berberine (50 mg/kg) 1 h before CS exposure. In the NanoBer + CS group, rats were intragastrically treated with the dispersion of Ber-encapsulated SLN-chitosan nanoparticles (containing 50 mg/kg) 1 hour before CS exposure. As previous investigations have shown that the berberine administration at a dose of approximately 50 mg/kg exerts a significant therapeutic impact on animal models

[18, 38–41], only one dosage (50 mg/kg) of berberine was administered in the present investigation to lessen the number of animals in accordance with the rules of animal ethics. The COPD rat model was developed according to previous reports with minor modifications [42–44]. Briefly, healthy rats were exposed to the CS of 12 3R4F research cigarettes in a chamber (100 × 70 × 35 cm) for 1 h daily, 6 days per week for 24 weeks. One day after the final CS exposure, animals were anesthetized by intraperitoneal injection of sodium pentobarbital (70 mg/kg). Arterial blood and the lung tissues were collected and stored at −80°C until the subsequent investigations. All animal investigations were conducted in accordance with the Guideline of the National Institute of Health for the Care and Use of Laboratory Animals and were approved by the animal ethical committee of the Affiliated Hospital of Hebei University (no. AHHU210416).

2.4. In Vivo Pharmacokinetic Study.
The formulations (aqueous suspension of berberine and dispersion of Ber-encapsulated SLN-chitosan nanoparticles) were administered in two groups of male SD rats ($n = 10$ per group) by intragastric gavage at an equivalent dose of berberine (50 mg/kg). The blood samples were dropped out from the tail vein into K3EDTA tubes at 0.25, 0.5, 1, 1.5, 3, 6, 9, 12, 18, and 24 h after dosing. The blood samples were then centrifuged at 3000 rpm for 8 min at 4°C, and the plasma samples were moved into 1.5 mL tubes and stored at −20°C until HPLC analysis [45].

2.5. Analyzing the Histopathology of Lung Tissue.
The left lobes of lung tissues were cut into 4 mm-thick slices and inflated with 4% paraformaldehyde for 48 h to permit the full fixation. Fixed samples were then immersed in paraffin (Sigma, USA) and cut into 4 μm-thick sections that were stained with hematoxylin and eosin (H&E) (Sigma, USA). A pathologist who was blinded to the group treatments analyzed histopathological alterations of tissues under a light inversion microscope (Leica Microsystems, Wetzlar, Germany). The grade of airway inflammation was scored on a 0–3 scale determined as 0 = no inflammation (normal); 1 = mild inflammation with the population of inflammatory cells in alveolar septa or bronchial; 2 = moderate inflammation with localized inflammation or patchy inflammation in walls of alveolar septa or bronchi in less than 1/3 of the lung cross-sectional area; 3 = severe inflammation with diffuse inflammatory cells in walls of alveoli septa or bronchi in 1/3 to 2/3 of the lung cross-sectional area [46]. Morphological parameters including the destructive index (DI) and mean linear intercept (MLI) were measured as previously explained [47]. The MLI parameter represents the changes in the air space size. The DI parameter indicates the percentage of collapsed space as a portion of the whole alveolus. MLI and DI were calculated by the following equations:

$$MLI = \frac{\text{length of a line drawn across the lung section}}{\text{total number of intercepts counted within this area}},$$

$$DI = \frac{\text{defined destructive alveoli}}{\text{total number of alveoli}}.$$

(1)

For statistical analysis, three microscopic fields were randomly checked in each slide.

2.6. Counting Inflammatory Cells in Bronchoalveolar Lavage Fluid (BALF).

The bronchoalveolar was lavaged 4 times with 1 ml saline buffer, with a 75%–85% recovery rate. The BALF samples were centrifuged for 4 min at 800 g and 4°C, and then the supernatants were removed and stored at −20°C for measurements of inflammatory cytokines. The BALF was then centrifuged for 8 minutes at 400 g and 4°C, and the cells were isolated for counting. Finally, the pelleted cells were resuspended in the saline buffer, and the total number of leukocytes was counted by Wright–Giemsa staining in accordance with the manufacturer's instructions (Beyotime Institute of Biotechnology, China) and using a standard hemocytometer. To classify the type of inflammatory cells, the differential cell count was employed by cytocentrifugation at 1400 g for 3 min and stained with Wright's stain.

2.7. Evaluating Levels of Inflammatory Mediators in BALF.

Levels of proinflammatory cytokines such as TNF-α, IL-1β, IL-6, and IL-8 in BALF were measured using commercially available enzyme-linked immunosorbent assay (ELISA) kits for rat cytokines (Elabscience Biotechnology Co., Ltd., China) in accordance with the manufacturer's instructions. The assays were performed in triplicate, and the optical density (OD) was measured at 450 nm by a microplate reader (Tecan, Männedorf, Switzerland).

2.8. Evaluating Activity of the Oxidant/Antioxidant System in BALF.

In order to evaluate the oxidant/antioxidant system, the enzymatic activities of myeloperoxidase (MPO) and superoxide dismutase (SOD) were measured in the BALF.

2.8.1. Measuring Myeloperoxidase Activity.

Myeloperoxidase (MPO) activity was assayed in the BALF samples using a colorimetric assay kit (ab105136) in accordance with the manufacturer's instructions. In brief, MPO catalyzes the formation of hypochlorous acid (HClO) from hydrogen peroxide (H_2O_2) and chloride ion (Cl^-). The hypochlorous acid rapidly reacts with taurine to produce the taurine chloramine, which subsequently reacts with the dianion 5-thio-2-nitrobenzoic acid (DTNB) probe to eliminate the color (absorbance at 412 nm). Finally, the MPO activity in the BALF samples was measured by comparison with the DTNB standard curve. The samples ($n = 10$) were assayed in triplicate, and the OD was measured at 412 nm using the microplate reader. The absorbance is inversely proportional to the MPO activity.

TABLE 1: The stability study of Ber-loaded SLN-chitosan nanoparticles at SIF and SGF.

Medium	Particle size (nm)		Encapsulation efficiency (%)	
	Initial	Final	Initial	Final
SIF (pH 6.8)	248.3 ± 9.7	259.5 ± 11.3	90.3 ± 3.4	82.6 ± 4.1
SGF (pH 1.5)	248.3 ± 9.7	261.4 ± 10.0	90.3 ± 3.4	73.7 ± 2.0

2.8.2. Measuring superoxide Dismutase Activity.

Superoxide dismutase (SOD) activity was evaluated in BALF samples using a colorimetric assay kit (ab65354) in accordance with the manufacturer's instructions. SOD detoxifies the superoxide anion (O_2^-) by converting this free radical to molecular oxygen (O_2) and hydrogen peroxide, thus providing cellular defense against ROS (24). Briefly, in the SOD assay protocol, superoxide anions are generated by the activity of xanthine oxidase. Then, generated superoxide anions converse to water-soluble formazan dye that can be assayed by the elevation in absorbance at 450 nm. The higher activity of SOD in the sample leads to less formazan generation. All assays were carried out in triplicate, and OD in all assays was measured at 450 nm using the microplate reader.

2.9. Statistical Analysis.

The normally and non-normally distributed data were expressed as mean ± standard deviation (SD) or median (25%–75% percentile), respectively. The significance of the difference between groups was determined by one-way ANOVA (on ranks) and Tukey–Kramer post-hoc multiple comparison test (GraphPad Prism software, version 8, San Diego, CA). Results with $p < 0.05$ were statistically regarded to be significant.

3. Results

3.1. Physiochemical Characterization of Ber-Encapsulated SLN-Chitosan Nanoparticles.

Ber-encapsulated SLN-chitosan nanoparticles exhibited narrow distribution width and notable narrow particle size, confirming the considerable dispersion quality (Figure 1(b)). In detail, the mean diameter, PDI, and surface charge were 255 ± 11 nm, 0.27 ± 0.09, and +29.3 ± 0.8 mV, respectively. The PDI value (<0.3) suggests a narrow particle size distribution [48]. The measurement of surface charge permits predicting the storage stability of colloidal particles since the charged particles show lesser aggregation than neutral particles. Ber-encapsulated SLN-chitosan nanoparticles possessed a positive surface charge that is desirable for reaching a stable formulation. This is ascribed to the presence of repulsive forces between nanoparticles, preventing particle contacting and agglomeration. Since chitosan possesses a positive charge because of the existence of the protonated amino groups, the positive surface charge of prepared nanoparticles also verified the coating of the chitosan polymer on the surface of SLNs. Figure 1(c) demonstrates the TEM micrograph of prepared Ber-encapsulated SLN-chitosan nanoparticles. The morphology of Ber-encapsulated SLN-chitosan
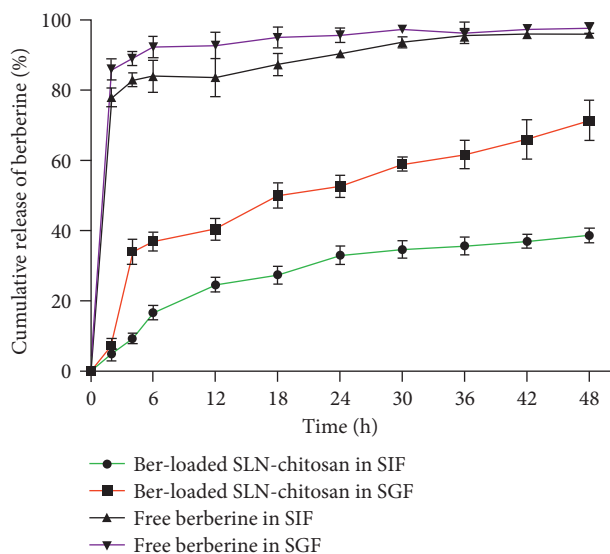
FIGURE 2: *In vitro* cumulative release profiles of free berberine and Ber-loaded SLN-chitosan nanoparticles in simulated gastric fluid (SGF, pH 1.5) and simulated intestinal fluid (SIF, pH 6.8).

nanoparticles indicated a spherical structure with a homogeneous size. Moreover, the EE% of berberine by chitosan-coated SLN nanoparticles was 90.3 ± 3.4%.

3.2. Stability of Ber-Encapsulated SLN-Chitosan Nanoparticles in Simulated Fluids. The stability was studied by adding Ber-encapsulated SLN-chitosan nanoparticles in SIF and SGF media. Ber-encapsulated SLN-chitosan nanoparticles were detected stable in both media (Table 1). Such stability can be due to the protective effect of multilayer coatings, which prevent the exposure of nanoparticles to the harsh environment of the gastrointestinal tract, suggesting the hardiness of the formulation. SLN layer provides a protective shield because of its resistance to digestive enzymes, while chitosan is able to protect the particle integrity and stability against acidic conditions.

3.3. In Vitro Drug Release. To simulate the *in vivo* physiological condition, the *in vitro* release studies were performed in SGF (pH 1.5) and SIF (pH 6.8) media. The controlled release profile of berberine from chitosan-coated SLNs in the two media is shown in Figure 2. Of note, the cumulative release of berberine from chitosan-coated nanoparticles was much slower than that of free berberine, which shows that these nanoparticles could effectively protect berberine in the harsh acidic condition of the gastrointestinal tract. Berberine was released from chitosan-coated SLNs by approximately 38% and 71% over 48 h in SGF and SIF, respectively. Of note, a biphasic release profile was found as an early burst release of berberine at the initiating phase, followed by a sustained release pattern at the late phase (during 48 h). Chitosan coating has been beneficial in further slowing the release rate [49]. The slow release of berberine in the SGF and SIF ensures that a sufficiently high concentration of Ber-encapsulated SLN-chitosan nanoparticles would be absorbed
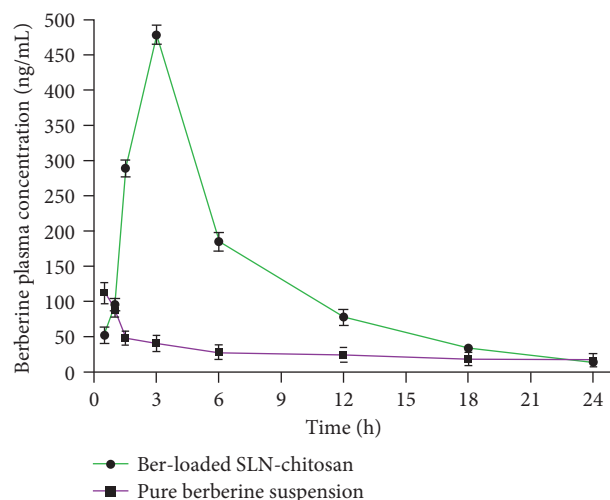

FIGURE 3: The profiles of the plasma concentration of berberine versus time after oral administration of Ber-loaded SLN-chitosan nanoparticles and the pure suspension of berberine in rats. Data are expressed as the mean ± SD ($n = 10$).

TABLE 2: Pharmacokinetic parameters in the treated rats after a single oral dose administration of Ber-loaded SLN-chitosan nanoparticles and pure suspension of berberine.

	Unit	Ber-loaded SLN-chitosan nanoparticles	Berberine
Dose	mg/kg	50	50
C_{max}	ng/ml	479 ± 13	112 ± 14
T_{max}	h	3	0.5
AUC	ng.h/ml	2973 ± 76	647 ± 77
BAR		—	4.6-fold

AUC, area under the berberine plasma concentration-time curve; BAR, the relative bioavailability of oral administration of Ber-loaded SLN-chitosan nanoparticles compared with the pure berberine suspension; C_{max}, the maximum plasma concentration of berberine after oral administration; T_{max}, the time to maximum plasma concentration of berberine.

by the small intestine. Thus, SLN-chitosan nanoparticles show a promising potential to provide a long-acting and efficient delivery platform to improve berberine absorption in the small intestine after oral administration.

3.4. In Vivo Pharmacokinetic Study. The plasma levels versus time profiles of berberine after oral administration of Ber-encapsulated SLN-chitosan nanoparticles and the pure suspension of berberine are shown in Figure 3. Table 2 summarizes the pharmacokinetic values of Ber-encapsulated SLN-chitosan nanoparticles obtained from the study. The C_{max} and T_{max} of Ber-encapsulated SLN-chitosan nanoparticles were detected to be 479 ± 13 ng/mL and 3 h, respectively. However, significantly lower C_{max} (112 ± 14 ng/mL) and T_{max} (0.5 h) were achieved with pure berberine. Moreover, a higher AUC_{0-t} (2973 ± 76 ng·h/mL) was obtained with Ber-encapsulated SLN-chitosan nanoparticles when compared with the pure berberine, which only obtained 647 ± 77 ng·h/mL. Moreover, a 4.6-fold elevation in
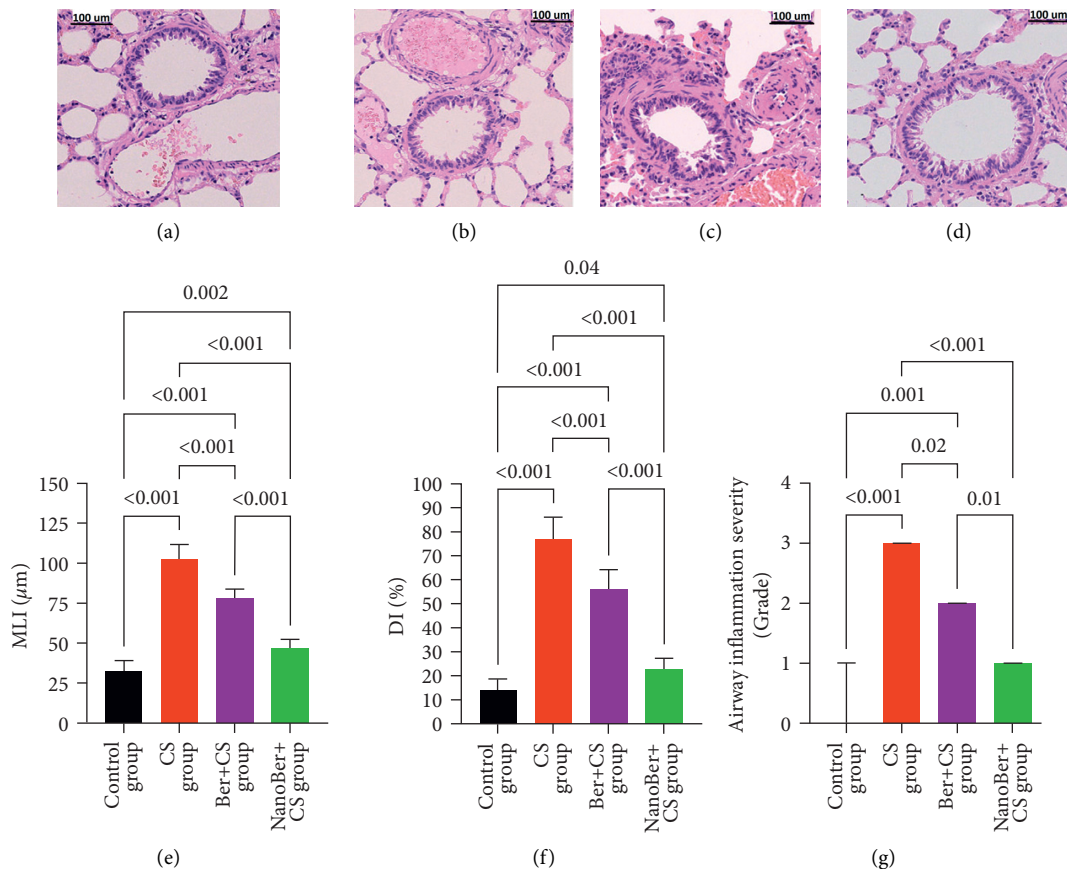
FIGURE 4: The effect of Ber-loaded SLN-chitosan nanoparticles and the pure suspension of berberine on CS-induced lung histological alterations. Representative H&E staining images of lung tissue sections from the control group. (a) CS group, (b) Ber + CS group, (c) NanoBer + CS group, (d) under an optical microscope (original magnification ×200, scale bar 100 μm). MLI ((e) and DI (f) values were calculated to estimate changes in the airway space size and structure. Data are expressed as mean ± SD ($n = 10$). The severity of airway inflammation was graded on a 0–3 scale. Data are expressed as median (25%–75% percentile) ($n = 10$) (g). Statistical analysis was carried out by one-way analysis of variance (ANOVA) followed by Tukey's multiple comparison test. $p < 0.05$ is considered as statistically significant.

relative bioavailability was obtained in the Ber-encapsulated SLN-chitosan group once compared with the pure berberine group. The delayed T_{max} with Ber-encapsulated SLN-chitosan nanoparticles indicated the sustained berberine release *in vivo*, which was in agreement with the results of *in vitro* release profiles.

3.5. *Histopathological Changes of Lung Tissues.* The H&E stained lung tissues are depicted in Figure 4. Compared with the control group (Figure 4(a)), the lung tissue of rats in the CS group manifested pathological features of COPD including alveolar enlargement and fusion, thinner alveolar septum and alveolar wall rupture, and infiltration of inflammatory cells, mainly alveolar macrophages and neutrophils (Figure 4(b)). Notably, such histopathological alterations were significantly improved by the pure berberine pretreatment (Figure 4(c)) and, to a higher extent, by the Ber-encapsulated SLN-chitosan pretreatment (Figure 4(d)) in CS-exposed rats. Quantitative analysis of lung tissue pathology indicated that MLI and DI in the CS group were significantly increased relative to the control group ($p < 0.001$, Figures 4(e) and 4(f)). Notably, MLI and

DI were significantly decreased in the Ber + CS group (by −24.1% and −26.8%, respectively, $p < 0.001$) and in the NanoBer + CS group (by −54.5% and −70.4%, respectively, $p < 0.001$) relative to the CS group. When compared with the Ber + CS group, MLI and DI were significantly decreased in the NanoBer + CS group by −39.8% and −59.6%, respectively, $p < 0.001$. Based on the intensity of inflammatory cell infiltration, the severity of airway inflammation was scored on a scale of 0–3 (Figure 4(g)). The median inflammation score was significantly elevated in the CS group (3 [2, 3]) relative to the control group (0 [0–0.25]) ($p < 0.001$). Such a CS-induced inflammation was significantly decreased in the Ber + CS group (2 [1–2]) and NanoBer + CS group (1 [0–1]) as compared with the CS group ($p < 0.02$ and $p < 0.001$, respectively). Notably, the NanoBer + CS group indicated a significantly lower median inflammation score than the Ber + CS group ($p < 0.01$).

3.6. *Levels of Inflammatory Cells in BALF.* The number of inflammatory cells was significantly elevated ($p < 0.001$) in the BALF of the CS group relative to the control group (Table 3). Notably, the administration of the pure berberine

TABLE 3: Inflammatory cell counts in BALF.

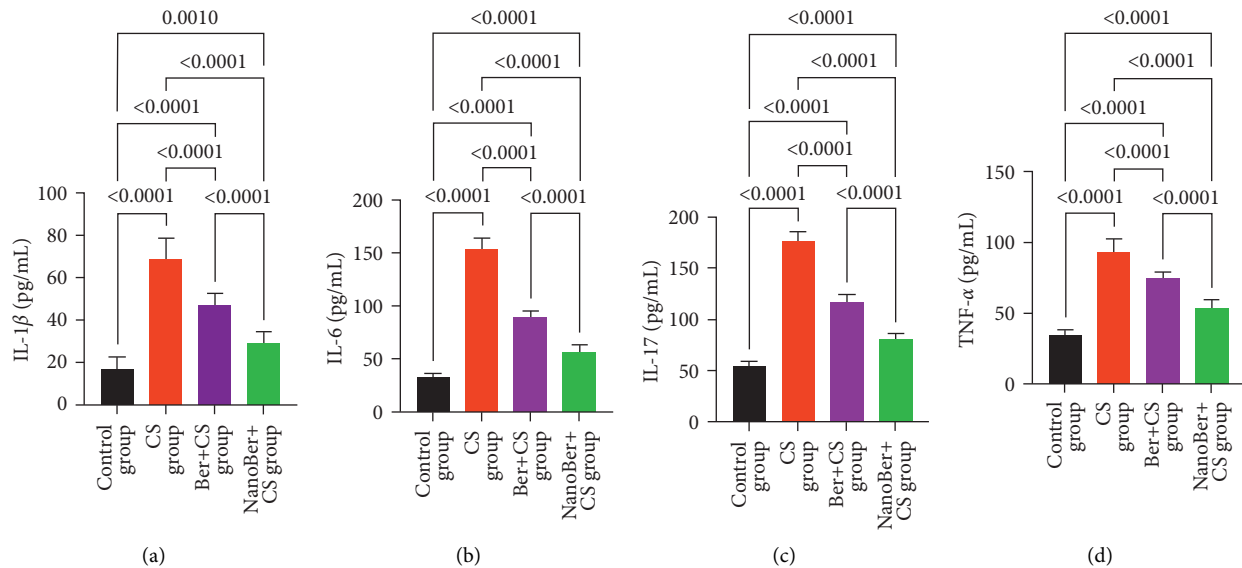|	Total leukocyte ($\times 10^5$ cells/mL)	Macrophage ($\times 10^5$ cells/mL)	Neutrophils ($\times 10^5$ cells/mL)
Control group	2.46 ± 0.32	1.62 ± 0.2	0.19 ± 0.1
CS group	19.4 ± 5.1	8.9 ± 1.4	6.9 ± 1.6
Ber + CS group	11.2 ± 1.3	5.9 ± 1.2	4.1 ± 0.6
NanoBer + CS group	6 ± 1.1	3 ± 0.9	2.23 ± 0.7

Data represent mean ± SD.

FIGURE 5: Effect of Ber-loaded SLN-chitosan nanoparticles and the pure suspension of berberine on inflammatory cytokines in BALF in CS-induced COPD rats. Data are expressed as mean ± SD ($n = 10$). Statistical analysis was carried out by one-way analysis of variance (ANOVA) followed by Tukey's multiple comparison test. $p < 0.05$ is considered as statistically significant.

suspension and Ber-encapsulated SLN-chitosan nanoparticles could significantly decrease counts of inflammatory cells in BALF of CS-exposed rats ($p < 0.001$). In detail, counts of total leukocyte, macrophages, and neutrophils in BALF of Ber + CS group and NanoBer + CS group were decreased by (−42.2%, −33.7%, and −40.5%) and (−69%, −66.3%, and −67.7%), respectively, relative to the CS group. When compared with the Ber + CS group, counts of total leukocytes, macrophages, and neutrophils were decreased by −46.4%, −49.1%, and −45.6% in BALF of the NanoBer + CS group ($p < 0.001$).

3.7. Levels of Proinflammatory Cytokines in BALF.

The levels of proinflammatory cytokines were evaluated in BALF using the ELISA method (Figure 5). The results demonstrated that the BALF levels of IL-1β, IL-6, IL-17, and TNF-α were significantly higher in the CS group than those in the control group ($p < 0.001$). Of note, the levels of IL-1β, IL-6, IL-17, and TNF-α were significantly decreased by (−31.25%, −41.72%, −33.76%, −20.61%, respectively) and (−57.38%, −62.97%, −54.37%, and −42.55%, respectively) in the Ber + CS group and the NanoBer + CS group, respectively, relative to the CS group ($p < 0.001$). When compared with the Ber + CS group, the levels of IL-1β, IL-6, IL-17, and TNF-α were significantly reduced by −38%, −36.46%, −31.11%, and −27.64%, respectively, in the NanoBer + CS group ($p < 0.001$).

3.8. Activity of the Oxidant/Antioxidant System in BALF.

As depicted in Figure 6, the MPO activity in BALF was significantly elevated in the CS group relative to the control group ($p < 0.0001$), while the SOD activity was significantly decreased ($p < 0.0001$). Notably, compared with CS group, BALF MPO in treatment groups Ber + CS and NanoBer + CS was significantly decreased by −49.5% ($p < 0.0001$) and −79.2 ($p < 0.0001$), respectively, whereas BALF SOD was significantly elevated by +39.8% ($p < 0.0003$) and +90.7% ($p < 0.0001$), respectively.

4. Discussion

The findings of the present study demonstrated that the encapsulation in chitosan-coated SLN nanoparticles could markedly enhance the oral bioavailability and therapeutic anti-inflammatory impacts of berberine in the CS-induced COPD rat model. The anti-inflammatory effects of berberine have been well documented by numerous studies in various inflammation-mediated diseases [11–17]. Similar to our results, other *in vivo* studies have been shown that the pretreatment with berberine could significantly suppress the release of inflammatory cytokines and inflammatory cells into BALF, which was accompanied with the prevention of CS-induced airway inflammation in mice [18–20].
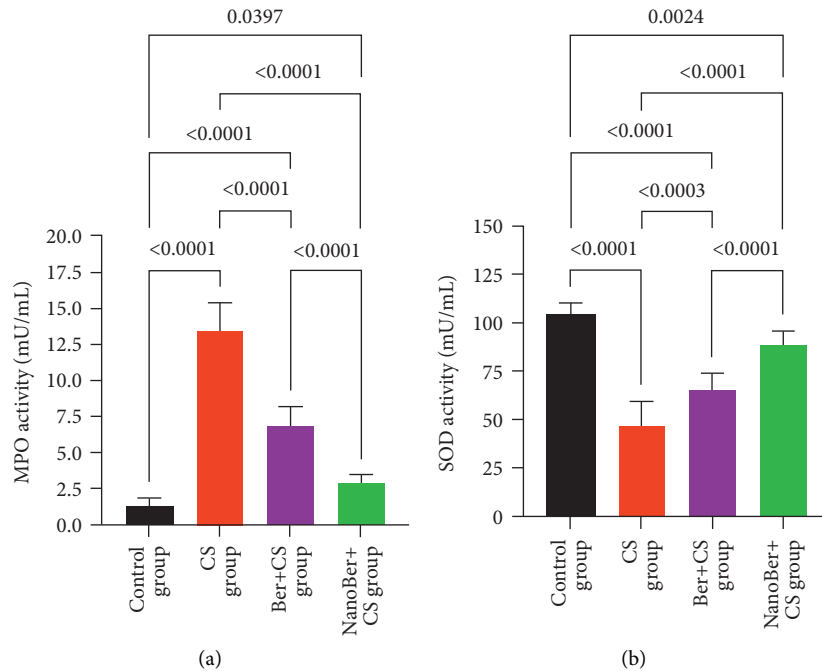
FIGURE 6: Effect of Ber-loaded SLN-chitosan nanoparticles and the pure suspension of berberine on the activity of MPO and SOD in BALF in CS-induced COPD rats. Data are expressed as mean ± SD ($n = 10$). Statistical analysis was carried out by one-way analysis of variance (ANOVA) followed by Tukey's multiple comparison test. $p < 0.05$ is considered as statistically significant.

Inflammation and oxidative stress are known to play a key role in COPD pathogenesis [50]. Neutrophils and macrophages are the main innate immune cells that infiltrate the lungs and participate in the pathogenesis of CS-induced COPD through inflammation and direct induction of endothelial and epithelial cell death [20, 51, 52]. Neutrophils have been detected to be increased in the small airways of COPD patients [53]. Inflammatory alveolar macrophages tend to express inflammatory cytokines and secrete matrix metalloproteases, and activated neutrophils are recruited to the airways and release reactive oxygen species (ROS) and neutrophil elastase, causing an injury to the epithelium and underlying basement membrane in the lung tissues and leading to COPD progression [20, 51, 52, 54]. Such inflammatory cells can also promote immune responses, leading to an elevation in levels of inflammatory cytokines, which intensify the inflammatory response and exert a key role in the airway inflammation in COPD by recruiting inflammatory cells and airway hyper-responsiveness [55–65]. Notably, IL-1β and TNFα are proinflammatory cytokines that are correlated with neutrophilic inflammation and macrophage activation, and their levels are increased in COPD and contribute to the pathogenesis of COPD [66]. TNF-α is majorly produced by macrophages, induces inflammatory cells recruitment, elevates the activity of proteolytic enzymes, and exacerbates mucus secretion and airflow limitation in COPD [57, 58, 67]. IL-1β has been found to be an important player in the promotion of emphysema and small airway remodeling in murine models [56, 68]. Moreover, IL-6 is another critical proinflammatory cytokine [69] that is considered as a COPD candidate mediator [59, 60] and can induce the development of COPD

in experimental animals [62]. The key role of IL-6 in airway inflammation can be further supported by clinical investigations showing elevated systemic levels of IL-6 in COPD patients [63–65]. Our results indicated that oral administration of Ber-encapsulated SLN-chitosan nanoparticles and pure berberine significantly prevented the CS-induced airway inflammation in rats, as detected by the reduction of inflammatory cell infiltration in lung tissues and decreased levels of proinflammatory cytokines (TNF-α, IL-1β, IL-6, and IL-17) and inflammatory cells (neutrophils and macrophages) in BALF. Importantly, we found that nanoparticle encapsulation could strongly enhance the preventive effect of berberine on the elevation of inflammatory cells and cytokines in BALF and lung tissues of CS-exposed rats.

Notably, CS and inflammatory cells are the main sources of oxidative stress in the lungs, as activated cells recruited to the airways generate excessive amounts of ROS, which leads to oxidation of nucleic acids, proteins, and lipids, causing tissue damage. Notably, the tissue damage results in the further recruitment of inflammatory cells to the lungs that, in turn, extends oxidative stress and eventually climaxes into a dangerous inflammatory cycle [70]. In addition, elevated levels of oxidative stress markers such as MPO, with a concomitant reduction in antioxidants like SOD [70], have been detected in COPD patients, showing an oxidant-antioxidant imbalance in these patients. MPO is a potent oxidant enzyme abundantly expressed in neutrophils, employs as a surrogate marker of neutrophilic inflammation, and plays an active role in CS-induced systemic inflammation [71]. Upon neutrophil activation, MPO is released from azurophilic granules and catalyzes the formation of powerful oxidants, such as hypochlorous acid, which are

able to oxidize by-products of CS, causing lung injury [70]. Of note, the MPO inhibition has been found to suppress the progression of CS-induced physiological alterations of COPD, such as emphysema and small airway and pulmonary arterial remodeling in animal models [72–74], supporting the role of MPO in COPD. Of note, our results indicated that berberine pretreatment could suppress MPO activity in CS-induced COPD rats, and such an effect was highly improved by Ber-encapsulated SLN-chitosan nanoparticles. Notably, the suppression of MPO activity by the berberine formulations was found to associate well with a reduction of neutrophils in the lung tissues. Thus, since MPO activity is an indicator of neutrophil infiltration and inflammation [75], this result further supports the neutrophil suppression by the berberine formulation in our study. Moreover, antioxidant enzymes can repair damaged cells and decrease injury. SOD is an anti-inflammatory enzyme as well as a major antioxidant that can scavenge superoxide radicals and prevent ROS-induced cell/tissue injury. The reduced level of SOD has been reported in plasma and BALF from animal models and COPD patients [43, 76–82]. Thus, SOD activity can indicate the degree of lung tissue damage in COPD. Our results indicated that pretreatment with the berberine formulations could strongly enhance the SOD activity in CS-induced COPD rats, in which Ber-encapsulated SLN-chitosan nanoparticles exerted a higher effect.

The better protection against CS-induced airway inflammation in COPD rats by Ber-encapsulated SLN-chitosan can be due to the enhanced oral bioavailability of berberine by chitosan-coated SLN nanoparticles. With encapsulation in SLN-chitosan nanoparticles, the peak plasma level of berberine in rats was increased, the peak time was postponed, and the AUC was elevated, showing an enhanced oral bioavailability of berberine. This higher bioavailability can be explained by the physicochemical properties of Ber-encapsulated SLN-chitosan nanoparticles. The *in vitro* tests indicated excellent stability in the simulated gastric condition (pH 1.5) and a sustained release profile in the simulated intestinal condition (pH 6.8), supporting the significantly higher bioavailability of Ber-encapsulated SLN-chitosan nanoparticles than the pure berberine by oral administration in rats. On the other hand, the prepared nanoparticles showed a small particle size <300 nm, which is desirable for being invisible to the reticuloendothelial system and for a long-time circulation in the bloodstream. In addition, these nanoparticles possessed a positive surface charge that makes them able to easily contact the negatively charged membrane of intestinal cells and, thereby, in contrast to the neutral and negatively charged particles, are more rapidly uptaken by the cell membrane [83]. In addition, the hydrophilic feature of chitosan coating can also strongly intensify the hydrogen bonds between the nanoparticles and the intestinal mucus layer and, thereby, improve mucoadhesion. This can be further supported by other studies that showed the elevated intestinal absorption of drugs encapsulated in chitosan-coated SLN nanoparticles, due to the ionic and hydrophilic interactions [30, 31]. Further, the size and shape have been found to directly impact the cellular uptake of nanoparticles [84]. As depicted by the TEM images, the prepared Ber-encapsulated SLN-chitosan nanoparticles figured a homogeneous spherical shape in nature. The size- and shape-dependent uptake of nanoparticles is attributed to a phenomenon termed membrane wrapping, which determines how a membrane can put in a particle [84, 85].

While the present study is the first to report the anti-inflammatory effect of a nanoformulation of berberine on COPD, a number of limitations need to be acknowledged to guide future studies. One of these limitations includes the need for the verification of results in additional models of COPD including those induced by lipopolysaccharide (LPS) or elastase. Additionally, in vivo toxicity studies and the biodistribution of the Ber-encapsulated SLN-chitosan nanoparticles in different organs such as the liver, kidneys, heart, and spleen should be evaluated. In vitro studies for evaluating intestinal uptake and mucoadhesive property of Ber-encapsulated SLN-chitosan nanoparticles are also needed.

5. Conclusion

In the present study, a novel self-assembled chitosan-coated SLN nanoparticle formulation for encapsulating berberine has been developed and its therapeutic potential was evaluated in CS-induced COPD rats. The stable and small nanoparticle size, the homogeneous morphological structure, the high EE, the excellent biological stability, and the sustained berberine release properties have been obtained. Upon oral administration to rats, the bioavailability of Ber-encapsulated SLN-chitosan was detected to have been significantly improved relative to that of the pure berberine suspension. *In vivo* investigations also successfully showed that using chitosan-coated SLN nanoparticles could improve the ameliorative effect of berberine on CS-induced airway inflammation in COPD rats. Of note, the high bioavailability of Ber-encapsulated SLN-chitosan can be an important reason contributing to the improvement of the therapeutic effect of berberine in CS-induced COPD rats. Overall, chitosan-coated SLN nanoparticles offer an excellent oral delivery platform to improve the aqueous solubility and the oral bioavailability of berberine and thereby facilitate its pharmacological activities.

Data Availability

The data used to support the findings of this study are included within the article.

Conflicts of Interest

The authors declare that they have no conflicts of interest.

Acknowledgments

References

[1] A. Agustí and J. C. Hogg, "Update on the pathogenesis of chronic obstructive pulmonary disease," *New England Journal of Medicine*, vol. 381, no. 13, pp. 1248–1256, 2019.

[2] S. T. Lugg, A. Scott, D. Parekh, B. Naidu, and D. R. Thickett, "Cigarette smoke exposure and alveolar macrophages: mechanisms for lung disease," *Thorax*, vol. 77, no. 1, pp. 94–101, 2022.

[3] L. C. Davis, E. Sapey, D. R. Thickett, and A. Scott, "Predicting the pulmonary effects of long-term e-cigarette use: are the clouds clearing?" *European Respiratory Review: An Official Journal of the European Respiratory Society*, vol. 31, no. 163, 2022.

[4] P. B. Gonçalves and N. C. Romeiro, "Multi-target natural products as alternatives against oxidative stress in chronic obstructive pulmonary disease (COPD)," *European Journal of Medicinal Chemistry*, vol. 163, pp. 911–931, 2019.

[5] Z. H. Saeed, M. A. Abd El Hakim, and N. R. Mohamed, "Chronic obstructive pulmonary disease in non-smokers: role of oxidative stress," *The Egyptian Journal of Bronchology*, vol. 15, no. 1, pp. 1–6, 2021.

[6] G. T. Ferguson, P. M. A. Calverley, J. A. Anderson et al., "Prevalence and progression of osteoporosis in patients with COPD," *Chest*, vol. 136, no. 6, pp. 1456–1465, 2009.

[7] D. T. Eurich, C. Lee, T. J. Marrie, and S. R. Majumdar, "Inhaled corticosteroids and risk of recurrent pneumonia: a population-based, nested case-control study," *Clinical Infectious Diseases*, vol. 57, no. 8, pp. 1138–1144, 2013.

[8] P. M. O'Byrne, S. Rennard, H. Gerstein et al., "Risk of new onset diabetes mellitus in patients with asthma or COPD taking inhaled corticosteroids," *Respiratory Medicine*, vol. 106, no. 11, pp. 1487–1493, 2012.

[9] Q.-M. Chen and M.-Z. Xie, "Studies on the hypoglycemic effect of coptis chinensis and berberine," *Yao Xue Xue Bao Acta Pharmaceutica Sinica*, vol. 21, no. 6, pp. 401–406, 1986.

[10] J. D. Keys, *Chinese Herbs*, Tuttle Publishing, Clarendon, VT, USA, 2011.

[11] S. M. Ehteshamfar, M. Akhbari, J. T. Afshari et al., "--Anti-inflammatory and immune-modulatory impacts of berberine on activation of autoreactive T cells in autoimmune inflammation," *Journal of Cellular and Molecular Medicine*, vol. 24, no. 23, pp. 13573–13588, 2020.

[12] S. Palai, *Berberine. Nutraceuticals and Health Care*, Elsevier, Clarendon, VT, USA, pp. 359–368, 2022.

[13] P. Shen, Y. Jiao, L. Miao, J. h. Chen, and A. A. Momtazi-Borojeni, "Immunomodulatory effects of berberine on the inflamed joint reveal new therapeutic targets for rheumatoid arthritis management," *Journal of Cellular and Molecular Medicine*, vol. 24, no. 21, pp. 12234–12245, 2020.

[14] A. Fatahian, S. M. Haftcheshmeh, S. Azhdari, H. K. Farshchi, B. Nikfar, and A. A. Momtazi-Borojeni, "Promising anti-atherosclerotic effect of berberine: evidence from in vitro, in vivo, and clinical studies," *Reviews of Physiology, Biochemistry & Pharmacology*, vol. 178, pp. 83–110, 2020.

[15] S. Mohammadian Haftcheshmeh and A. A. Momtazi-Borojeni, "-Berberine as a promising natural compound for the treatment of periodontal disease: a focus on anti-inflammatory properties," *Journal of Cellular and Molecular Medicine*, vol. 25, no. 24, pp. 11333–11337, 2021.

[16] S. H. Ayati, B. Fazeli, A. A. Momtazi-Borojeni, A. F. G. Cicero, M. Pirro, and A. Sahebkar, "Regulatory effects of berberine on microRNome in cancer and other conditions," *Critical Reviews in Oncology*, vol. 116, pp. 147–158, 2017.

[17] H. Mortazavi, B. Nikfar, S.-A. Esmaeili et al., "Potential cytotoxic and anti-metastatic effects of berberine on gynaecological cancers with drug-associated resistance," *European Journal of Medicinal Chemistry*, vol. 187, Article ID 111951, 2020.

[18] W. Wang, G. Zha, J.-j. Zou, X. Wang, C.-N. Li, and X.-J. Wu, "Berberine attenuates cigarette smoke extract-induced airway inflammation in mice: involvement of TGF-β1/smads signaling pathway," *Current medical science*, vol. 39, no. 5, pp. 748–753, 2019.

[19] K. Lin, S. Liu, Y. Shen, and Q. Li, "Berberine attenuates cigarette smoke-induced acute lung inflammation," *Inflammation*, vol. 36, no. 5, pp. 1079–1086, 2013.

[20] D. Xu, C. Wan, T. Wang et al., "Berberine attenuates cigarette smoke-induced airway inflammation and mucus hypersecretion in mice," *International Journal of Clinical and Experimental Medicine*, vol. 8, no. 6, pp. 8641–8647, 2015.

[21] W. Hua, L. Ding, Y. Chen, B. Gong, J. He, and G. Xu, "Determination of berberine in human plasma by liquid chromatography-electrospray ionization-mass spectrometry," *Journal of Pharmaceutical and Biomedical Analysis*, vol. 44, no. 4, pp. 931–937, 2007.

[22] F. Zuo, N. Nakamura, T. Akao, and M. Hattori, "Pharmacokinetics of berberine and its main metabolites in conventional and pseudo germ-free rats determined by liquid chromatography/ion trap mass spectrometry," *Drug Metabolism and Disposition*, vol. 34, no. 12, pp. 2064–2072, 2006.

[23] Y.-T. Liu, H.-P. Hao, H.-G. Xie et al., "Extensive intestinal first-pass elimination and predominant hepatic distribution of berberine explain its low plasma levels in rats," *Drug Metabolism and Disposition*, vol. 38, no. 10, pp. 1779–1784, 2010.

[24] S. K. Battu, M. A. Repka, S. Maddineni, A. G. Chittiboyina, M. A. Avery, and S. Majumdar, "Physicochemical characterization of berberine chloride: a perspective in the development of a solution dosage form for oral delivery," *AAPS Pharmacy Science Technology*, vol. 11, no. 3, pp. 1466–1475, 2010.

[25] J. L. Madara, "Loosening tight junctions. Lessons from the intestine," *Journal of Clinical Investigation*, vol. 83, no. 4, pp. 1089–1094, 1989.

[26] C.-S. Liu, Y.-R. Zheng, Y.-F. Zhang, and X.-Y. Long, "Research progress on berberine with a special focus on its oral bioavailability," *Fitoterapia*, vol. 109, pp. 274–282, 2016.

[27] C. Chen, T. Fan, Y. Jin et al., "Orally delivered salmon calcitonin-loaded solid lipid nanoparticles prepared by micelle-double emulsion method via the combined use of different solid lipids," *Nanomedicine*, vol. 8, no. 7, pp. 1085–1100, 2013.

[28] M. George and T. E. Abraham, "Polyionic hydrocolloids for the intestinal delivery of protein drugs: alginate and chitosan—a review," *Journal of Controlled Release*, vol. 114, no. 1, pp. 1–14, 2006.

[29] I. A. Sogias, A. C. Williams, and V. V. Khutoryanskiy, "Why is chitosan mucoadhesive?" *Biomacromolecules*, vol. 9, no. 7, pp. 1837–1842, 2008.

[30] Y. Luo, Z. Teng, Y. Li, and Q. Wang, "Solid lipid nanoparticles for oral drug delivery: chitosan coating improves stability, controlled delivery, mucoadhesion and cellular uptake," *Carbohydrate Polymers*, vol. 122, pp. 221–229, 2015.

[31] P. Fonte, T. Nogueira, C. Gehm, D. Ferreira, and B. Sarmento, "Chitosan-coated solid lipid nanoparticles enhance the oral absorption of insulin," *Drug Delivery and Translational Research*, vol. 1, no. 4, pp. 299–308, 2011.

[32] R. Nair, A. C. Kumar, V. K. Priya, C. M. Yadav, and P. Y. Raju, "Formulation and evaluation of chitosan solid lipid nanoparticles of carbamazepine," *Lipids in Health and Disease*, vol. 11, no. 1, pp. 72–78, 2012.

[33] D. M. Ridolfi, P. D. Marcato, G. Z. Justo, L. Cordi, D. Machado, and N. Durán, "Chitosan-solid lipid nanoparticles as carriers for topical delivery of tretinoin," *Colloids and Surfaces B: Biointerfaces*, vol. 93, pp. 36–40, 2012.

[34] F. Q. Hu, S. P. Jiang, Y. Z. Du, H. Yuan, Y. Q. Ye, and S. Zeng, "Preparation and characterization of stearic acid nanostructured lipid carriers by solvent diffusion method in an aqueous system," *Colloids and Surfaces. B, Biointerfaces*, vol. 45, no. 3-4, pp. 167–173, 2005.

[35] B. Sarmento, D. Mazzaglia, M. C. Bonferoni, A. P. Neto, M. do Céu Monteiro, and V. Seabra, "Effect of chitosan coating in overcoming the phagocytosis of insulin loaded solid lipid nanoparticles by mononuclear phagocyte system," *Carbohydrate Polymers*, vol. 84, no. 3, pp. 919–925, 2011.

[36] P. Ahmaditabar, A. A. Momtazi-Borojeni, A. H. Rezayan, M. Mahmoodi, A. Sahebkar, and M. Mellat, "Enhanced entrapment and improved in vitro controlled release of N-acetyl cysteine in hybrid PLGA/lecithin nanoparticles prepared using a nanoprecipitation/self-assembly method," *Journal of Cellular Biochemistry*, vol. 118, no. 12, pp. 4203–4209, 2017.

[37] A. K. Anal and W. F. Stevens, "Chitosan–alginate multilayer beads for controlled release of ampicillin," *International Journal of Pharmaceutics*, vol. 290, no. 1-2, pp. 45–54, 2005.

[38] Y. Zhou, S.-q. Liu, H. Peng, L. Yu, B. He, and Q. Zhao, "In vivo anti-apoptosis activity of novel berberine-loaded chitosan nanoparticles effectively ameliorates osteoarthritis," *International Immunopharmacology*, vol. 28, no. 1, pp. 34–43, 2015.

[39] S.-J. Wu, T.-M. Don, C.-W. Lin, and F.-L. Mi, "Delivery of berberine using chitosan/fucoidan-taurine conjugate nanoparticles for treatment of defective intestinal epithelial tight junction barrier," *Marine Drugs*, vol. 12, no. 11, pp. 5677–5697, 2014.

[40] M. Xue, L. Zhang, M. Yang et al., "Berberine-loaded solid lipid nanoparticles are concentrated in the liver and ameliorate hepatosteatosis in db/db mice," *International Journal of Nanomedicine*, vol. 10, p. 5049, 2015.

[41] M. Xue, M.-X. Yang, W. Zhang et al., "Characterization, pharmacokinetics, and hypoglycemic effect of berberine loaded solid lipid nanoparticles," *International Journal of Nanomedicine*, vol. 8, p. 4677, 2013.

[42] H. Zhang, B. Liu, S. Jiang et al., "Baicalin ameliorates cigarette smoke-induced airway inflammation in rats by modulating HDAC2/NF-κB/PAI-1 signalling," *Pulmonary Pharmacology and Therapeutics*, vol. 70, Article ID 102061, 2021.

[43] W. Shen, J. Liu, M. Fan et al., "MiR-3202 protects smokers from chronic obstructive pulmonary disease through inhibiting FAIM2: an in vivo and in vitro study," *Experimental Cell Research*, vol. 362, no. 2, pp. 370–377, 2018.

[44] Q. Li, J. Sun, N. Mohammadtursun, J. Wu, J. Dong, and L. Li, "Curcumin inhibits cigarette smoke-induced inflammation via modulating the PPARγ-NF-κB signaling pathway," *Food and Function*, vol. 10, no. 12, pp. 7983–7994, 2019.

[45] N. M. Khalil, T. C. F. d. Nascimento, D. M. Casa et al., "Pharmacokinetics of curcumin-loaded PLGA and PLGA-PEG blend nanoparticles after oral administration in rats," *Colloids and Surfaces B: Biointerfaces*, vol. 101, pp. 353–360, 2013.

[46] K. Triantaphyllopoulos, F. Hussain, M. Pinart et al., "A model of chronic inflammation and pulmonary emphysema after multiple ozone exposures in mice," *American Journal of Physiology—Lung Cellular and Molecular Physiology*, vol. 300, no. 5, pp. L691–L700, 2011.

[47] A. A. Robbesom, E. M. M. Versteeg, J. H. Veerkamp et al., "Morphological quantification of emphysema in small human lung specimens: comparison of methods and relation with clinical data," *Modern Pathology*, vol. 16, no. 1, pp. 1–7, 2003.

[48] Y. Luo, Y. Zhang, K. Pan, F. Critzer, P. M. Davidson, and Q. Zhong, "Self-emulsification of alkaline-dissolved clove bud oil by whey protein, gum Arabic, lecithin, and their combinations," *Journal of Agricultural and Food Chemistry*, vol. 62, no. 19, pp. 4417–4424, 2014.

[49] P. Ganesan, P. Ramalingam, G. Karthivashan, Y. T. Ko, and D.-K. Choi, "Recent developments in solid lipid nanoparticle and surface-modified solid lipid nanoparticle delivery systems for oral delivery of phyto-bioactive compounds in various chronic diseases," *International Journal of Nanomedicine*, vol. 13, pp. 1569–1583, 2018.

[50] M. C. Ferrera, W. W. Labaki, and M. K. Han, "Advances in chronic obstructive pulmonary disease," *Annual Review of Medicine*, vol. 72, no. 1, pp. 119–134, 2021.

[51] M.-A. Man, L. Davidescu, N.-S. Motoc et al., "Diagnostic value of the neutrophil-to-lymphocyte ratio (NLR) and platelet-to-lymphocyte ratio (PLR) in various respiratory diseases: a retrospective analysis," *Diagnostics and Traitements*.vol. 12, no. 1, p. 81, 2022.

[52] A. Tajbakhsh, S. M. Gheibihayat, D. Mortazavi et al., "The effect of cigarette smoke exposure on efferocytosis in chronic obstructive pulmonary disease; molecular mechanisms and treatment opportunities," *COPD: Journal of Chronic Obstructive Pulmonary Disease*, vol. 18, pp. 1–14, 2021.

[53] C. Pilette, B. Colinet, R. Kiss et al., "Increased galectin-3 expression and intra-epithelial neutrophils in small airways in severe COPD," *European Respiratory Journal*, vol. 29, no. 5, pp. 914–922, 2007.

[54] S. Kim and J. A. Nadel, "Role of neutrophils in mucus hypersecretion in COPD and implications for therapy," *Treatments in Respiratory Medicine*, vol. 3, no. 3, pp. 147–159, 2004.

[55] T. Shi and L. Feng, "Blood biomarkers associated with acute type II respiratory failure in COPD: a meta-analysis," *The Clinical Respiratory Journal*, vol. 16, 2022.

[56] A. Churg, S. Zhou, X. Wang, R. Wang, and J. L. Wright, "The role of interleukin-1β in murine cigarette smoke-induced emphysema and small airway remodeling," *American Journal of Respiratory Cell and Molecular Biology*, vol. 40, no. 4, pp. 482–490, 2009.

[57] S. Yu, X. Gao, and Z. Yan, "Relationship between gene polymorphisms of tumor necrosis factor-α-308 and phenotypes of acute exacerbation of chronic obstructive pulmonary diseases," *Chinese Journal of Tuberculosis and Respiratory Diseases*, vol. 39, no. 3, pp. 203–207, 2016.

[58] C.-H. Chiang, C.-H. Chuang, and S.-L. Liu, "Transforming growth factor-β1 and tumor necrosis factor-α are associated with clinical severity and airflow limitation of COPD in an additive manner," *Lung*, vol. 192, no. 1, pp. 95–102, 2014.

[59] D. G. Yanbaeva, M. A. Dentener, M. A. Spruit et al., "IL6 and CRP haplotypes are associated with COPD risk and systemic inflammation: a case-control study," *BMC Medical Genetics*, vol. 10, no. 1, pp. 23–11, 2009.

[60] T.-M. Lee, M.-S. Lin, and N.-C. Chang, "Usefulness of C-reactive protein and interleukin-6 as predictors of outcomes in patients with chronic obstructive pulmonary disease receiving pravastatin," *The American Journal of Cardiology*, vol. 101, no. 4, pp. 530–535, 2008.

[61] A. B. Roos and M. R. Stampfli, "Targeting Interleukin-17 signalling in cigarette smoke-induced lung disease: mechanistic concepts and therapeutic opportunities," *Pharmacology & Therapeutics*, vol. 178, pp. 123–131, 2017.

[62] S. M. Ruwanpura, L. McLeod, A. Miller et al., "Interleukin-6 promotes pulmonary emphysema associated with apoptosis in mice," *American Journal of Respiratory Cell and Molecular Biology*, vol. 45, no. 4, pp. 720–730, 2011.

[63] R. Ferrari, S. E. Tanni, L. M. Caram, C Corrêa, C. R Corrêa, and I Godoy, "Three-year follow-up of Interleukin 6 and C-reactive protein in chronic obstructive pulmonary disease," *Respiratory Research*, vol. 14, no. 1, pp. 24–27, 2013.

[64] R. Liang, W. Zhang, and Y.-M. Song, "Levels of leptin and IL-6 in lungs and blood are associated with the severity of chronic obstructive pulmonary disease in patients and rat models," *Molecular Medicine Reports*, vol. 7, no. 5, pp. 1470–1476, 2013.

[65] S. Bozinovski, A. Hutchinson, M. Thompson et al., "Serum amyloid a is a biomarker of acute exacerbations of chronic obstructive pulmonary disease," *American Journal of Respiratory and Critical Care Medicine*, vol. 177, no. 3, pp. 269–278, 2008.

[66] P. J. Barnes, "Targeting cytokines to treat asthma and chronic obstructive pulmonary disease," *Nature Reviews Immunology*, vol. 18, no. 7, pp. 454–466, 2018.

[67] J. Ryu, H. J. Lee, S. H. Park et al., "Effect of prunetin on TNF-α-induced MUC5AC mucin gene expression, production, degradation of IκB and translocation of NF-κB p65 in human airway epithelial cells," *Tuberculosis and Respiratory Diseases*, vol. 75, no. 5, pp. 205–209, 2013.

[68] B. Singh, S. Arora, and V. Khanna, "Association of severity of COPD with IgE and interleukin-1 beta," *Monaldi archives for chest diseas = Archivio Monaldi per le malattie del torace*, vol. 73, 2010.

[69] W. L. Biffl, E. E. Moore, F. A. Moore, C. C. Barnett Jr., and V. S. Carl, "Interleukin-6 delays neutrophil apoptosis," *Archives of Surgery*, vol. 131, no. 1, pp. 24–30, 1996.

[70] E. Zinellu, A. Zinellu, A. G. Fois et al., "Oxidative stress biomarkers in chronic obstructive pulmonary disease exacerbations: a systematic review," *Antioxidants*, vol. 10, no. 5, p. 710, 2021.

[71] K. Andelid, B. Bake, S. Rak, A. Lindén, A. Rosengren, and A. Ekberg-Jansson, "Myeloperoxidase as a marker of increasing systemic inflammation in smokers without severe airway symptoms," *Respiratory Medicine*, vol. 101, no. 5, pp. 888–895, 2007.

[72] E. Singla, G. Puri, V. Dharwal, and A. S. Naura, "Gallic acid ameliorates COPD-associated exacerbation in mice," *Molecular and Cellular Biochemistry*, vol. 476, no. 1, pp. 293–302, 2021.

[73] A. Churg, C. V. Marshall, D. D. Sin et al., "Late intervention with a myeloperoxidase inhibitor stops progression of experimental chronic obstructive pulmonary disease," *American Journal of Respiratory and Critical Care Medicine*, vol. 185, no. 1, pp. 34–43, 2012.

[74] S. Onoue, T. Matsui, Y. Aoki et al., "Self-assembled micellar formulation of chafuroside a with improved anti-inflammatory effects in experimental asthma/COPD-model rats," *European Journal of Pharmaceutical Sciences: Official Journal of the European Federation for Pharmaceutical Sciences*, vol. 45, no. 1-2, pp. 184–189, 2012.

[75] A. Zhu, D. Ge, J. Zhang et al., "Sputum myeloperoxidase in chronic obstructive pulmonary disease," *European Journal of Medical Research*, vol. 19, no. 1, pp. 12–11, 2014.

[76] M. Zhang, Y. Zhang, M. Roth et al., "Sirtuin 3 inhibits airway epithelial mitochondrial oxidative stress in cigarette smoke-induced COPD," *Oxidative Medicine and Cellular Longevity*, vol. 2020, Article ID 7582980, 12 pages, 2020.

[77] Y. Li, Y.-G. Tian, J.-S. Li et al., "Bufei Yishen granules combined with acupoint sticking therapy suppress oxidative stress in chronic obstructive pulmonary disease rats: via regulating peroxisome proliferator-activated receptor-gamma signaling," *Journal of Ethnopharmacology*, vol. 193, pp. 354–361, 2016.

[78] M. Ismail, M. F. Hossain, A. R. Tanu, and H. U Shekhar, "Effect of spirulina intervention on oxidative stress, antioxidant status, and lipid profile in chronic obstructive pulmonary disease patients," *BioMed Research International*, vol. 2015, 7 pages, Article ID 486120, 2015.

[79] X.-L. Wang, T. Li, J.-H. Li, S.-Y. Miao, and X.-Z. Xiao, "The effects of resveratrol on inflammation and oxidative stress in a rat model of chronic obstructive pulmonary disease," *Molecules*, vol. 22, no. 9, p. 1529, 2017.

[80] M. Zeng, Y. Li, Y. Jiang, G. Lu, X. Huang, and K. Guan, "Local and systemic oxidative stress and glucocorticoid receptor levels in chronic obstructive pulmonary disease patients," *Canadian Respiratory Journal*, vol. 20, 7 pages, Article ID 985382, 2013.

[81] G. Wang, N. Mohammadtursun, Y. Lv, H. Zhang, J. Sun, and J. Dong, "Baicalin exerts anti-airway inflammation and anti-remodelling effects in severe stage rat model of chronic obstructive pulmonary disease," *Evidence-based Complementary and Alternative Medicine*, vol. 201814 pages, 2018.

[82] X. Tian, Y. Xue, G. Xie et al., "(−)-Epicatechin ameliorates cigarette smoke-induced lung inflammation via inhibiting ROS/NLRP3 inflammasome pathway in rats with COPD," *Toxicology and Applied Pharmacology*, vol. 429, Article ID 115674, 2021.

[83] P. R. Lockman, M. O. Oyewumi, J. M. Koziara, K. E. Roder, R. J. Mumper, and D. D. Allen, "Brain uptake of thiamine-coated nanoparticles," *Journal of Controlled Release*, vol. 93, no. 3, pp. 271–282, 2003.

[84] A. Albanese, P. S. Tang, and W. C. W. Chan, "The effect of nanoparticle size, shape, and surface chemistry on biological systems," *Annual Review of Biomedical Engineering*, vol. 14, no. 1, pp. 1–16, 2012.

[85] S. E. A. Gratton, P. A. Ropp, P. D. Pohlhaus et al., "The effect of particle design on cellular internalization pathways," *Proceedings of the National Academy of Sciences*, vol. 105, no. 33, pp. 11613–11618, 2008.